THE JOURNAL OF PHYSICAL CHEMISTRY Letters

Letter

pubs.acs.org/JPCL

Mode-Specific S_N2 Reaction Dynamics

Yan Wang,[†,‡,⊥] Hongwei Song,[†,⊥] István Szabó,[§] Gábor Czakó,[*,§] Hua Guo,[*,∥] and Minghui Yang[*,†]

[†]Key Laboratory of Magnetic Resonance in Biological Systems, National Center for Magnetic Resonance in Wuhan, State Key Laboratory of Magnetic Resonance and Atomic and Molecular Physics, Wuhan Institute of Physics and Mathematics, Chinese Academy of Sciences, Wuhan 430071, China

[‡]School of Chemical and Environmental Engineering, Hubei University for Nationalities, Enshi 445000, China

[§]Department of Physical Chemistry and Materials Science, Institute of Chemistry, University of Szeged, Rerrich Béla tér 1, Szeged H-6720, Hungary

[∥]Department of Chemistry and Chemical Biology, University of New Mexico, Albuquerque, New Mexico 87131, United States

Supporting Information

ABSTRACT: Despite its importance in chemistry, the microscopic dynamics of bimolecular nucleophilic substitution (S_N2) reactions is still not completely elucidated. In this publication, the dynamics of a prototypical S_N2 reaction ($F^- + CH_3Cl \rightarrow CH_3F + Cl^-$) is investigated using a high-dimensional quantum mechanical model on an accurate potential energy surface (PES) and further analyzed by quasi-classical trajectories on the same PES. While the indirect mechanism dominates at low collision energies, the direct mechanism makes a significant contribution. The reactivity is found to depend on the specific reactant vibrational mode excitation. The mode specificity, which is more prevalent in the direct reaction, is rationalized by a transition-state-based model.

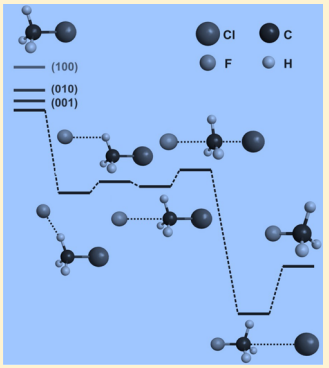

Concerted bimolecular nucleophilic substitution (S_N2) reactions with a carbon center, $X^- + CH_3Y \rightarrow CH_3X + Y^-$, particularly those with halogen ions X^- and Y^- as nucleophiles and leaving groups, play an important role in organic and biological chemistry.[1] However, the intrinsic dynamics of such reactions in solutions is difficult to investigate because solvent exerts a strong influence. Much experimental attention has thus been focused on the kinetics and dynamics of "naked" S_N2 reactions in the gas phase, where the energy can be controlled and product states characterized.[2−5] A better understanding of these isolated prototypes also helps to unravel the role played by solvent.

The recent molecular beam experiments in Wester's group have revealed unprecedented details on these prototypical S_N2 reactions.[6−9] With the help of atomistic simulations,[10−16] these observations have shed new light on the dynamics and microscopic mechanisms of these reactions. It is well recognized that the canonical Walden-inversion pathway features a prereaction ion−dipole complex $X^-\cdots CH_3Y$, a (often submerged) central barrier, and a postreaction ion−dipole complex $XCH_3\cdots Y^-$.[17,18] In addition, other less intuitive reaction pathways have also been found.[5,14] These microscopic mechanisms, some direct and others indirect, operate in different systems and energy ranges. As commented recently by Xie and Hase,[19] the intrinsic dynamics of these paradigm organic reactions is much more complex than expected.

Given the deep pre- and postreaction wells flanking the central barrier, it is tempting to assume that S_N2 reactions are statistical.[20] However, ample theoretical evidence has suggested otherwise due apparently to the slow intramolecular vibrational energy redistribution (IVR) in the reaction intermediates.[20−22] Nonstatistical behaviors have indeed been found in experiments.[23−29] One important characteristic of nonstatistical reactions is related to mode specificity, that is, the dependence of reactivity on the excitation of different reactant vibrational modes. As discussed intensively in the literature,[30−34] the reactivity in the statistical limit depends only on the amount of energy, rather than the specific form of the energy. So far, mode specificity has been almost exclusively found in activated reactions with explicit barriers, and a very few mode-specific barrierless reactions have been identified.[35,36] However, mode specificity has been predicted for S_N2 reactions,[14,37,38] although no experimental verification has so far been reported. In this work, we investigate, on an accurate potential energy surface (PES), mode specificity in a prototypical S_N2 reaction ($F^- + CH_3Cl \rightarrow CH_3F + Cl^-$) and its dependence on the reaction mechanism.

Although quasi-classical trajectory (QCT) methods[39] have been routinely used to study mode specificity in reactions, its approximate treatment of quantum effects such as zero-point energy and tunneling introduces some uncertainty in the outcomes. A related deficiency of QCT is its unphysically fast

Received: July 1, 2016
Accepted: August 9, 2016

DOI: 10.1021/acs.jpclett.6b01457
J. Phys. Chem. Lett. 2016, 7, 3322−3327

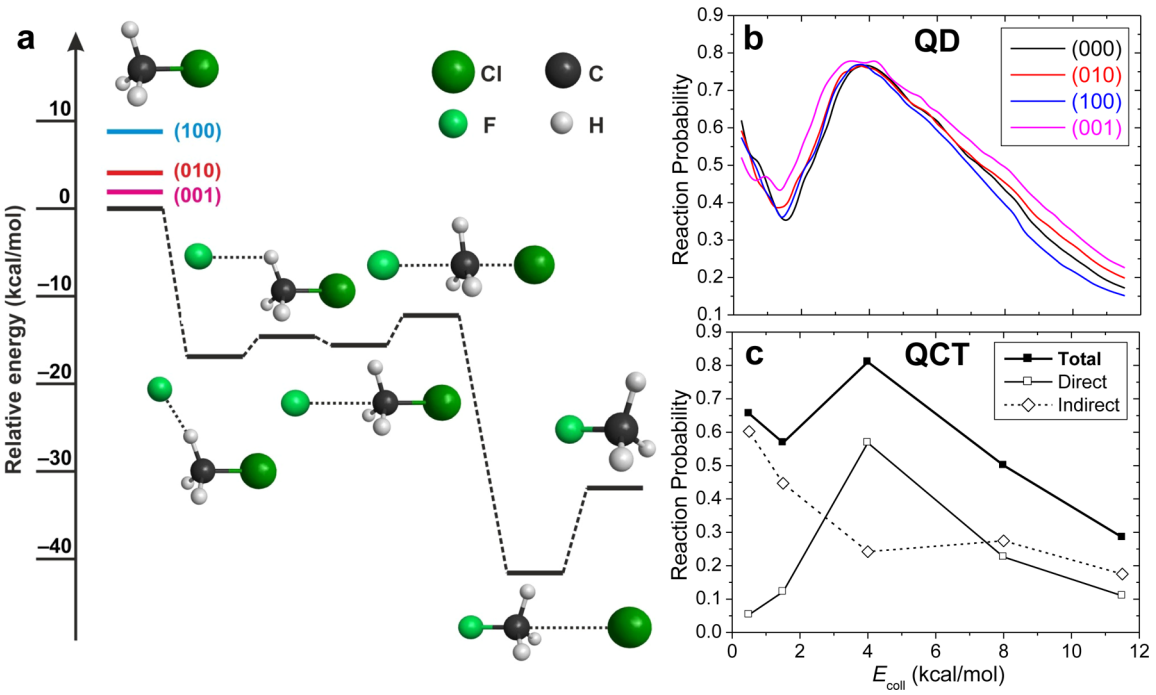

Figure 1. (a) Walden-inversion reaction pathway, (b) mode-specific QD, and (c) mechanism-specific ground-state QCT reaction probabilities (J_{tot} = 0) as a function of collision energy for the F^- + CH_3Cl S_N2 reaction.

rate of IVR for long-lived reaction complexes because of the lack of vibrational quantization in classical mechanics.[22] For these reasons, quantum mechanical treatment is essential for quantitative characterization of the mode-specific reaction dynamics. However, the large number of internal coordinates, heavy masses, and the relatively long reaction time have hampered realistic quantum dynamical (QD) studies.[38] So far, QD models for S_N2 reactions have been restricted to collinear geometry with at most four degrees of freedom (DOFs).[40−50] These models are not expected to give a realistic description of S_N2 reactions, which take place also at nonlinear geometries and involve more active DOFs.

In this work, we propose the first high-dimensional QD model for X^- + CH_3Y → CH_3X + Y^-, which includes six DOFs (6D) that are most relevant to the reaction. On the basis of the earlier model of Palma and Clary,[51] the entire CH_3Y moiety is assumed to maintain C_{3v} symmetry during the reaction. In addition to the scattering coordinate, the C−Y stretching, CH_3 symmetric stretching, and umbrella bending modes as well as the rotational DOFs of CH_3Y are included. This model is capable of describing not only the direct rebound but also direct stripping as well as the indirect mechanism, as defined by Hase and co-workers.[5] Because the YCH_3 moiety is allowed to rotate, it should provide a much more realistic description of the reaction dynamics than previous reduced-dimensional models, particularly at large impact parameters. We note in passing that this 6D model involves fewer DOFs than previous 7D or 8D studies of the X + CY_4/CYZ_3 type reactions,[52−58] but a 7D/8D treatment of this S_N2 reaction is currently infeasible due to the large basis set and long propagation time required to converge the results.

Despite some earlier work,[29,59−62] it was only very recently that the dynamics of this reaction was studied on a quantitative basis,[9,13,14,16,63] thanks to an accurate full-dimensional global PES.[14] This PES was fitted to about 50 000 high-level ab initio energy points over a large configuration space, in which the pre- and postreaction ion−dipole complexes, the C_s hydrogen-bonded complex, the transition states for both the Walden-inversion and front−side attack, the novel double-inversion pathway, and the proton-abstraction mechanism were all accurately described. In Figure 1a, the reaction path for the canonical Walden-inversion pathway is shown for this exothermic reaction, featuring a submerged barrier flanked by the ion−dipole wells. The dynamics of the title reaction is explored on the PES by performing time-dependent wave packet calculations within the 6D model. This is complemented with full-dimensional QCT calculations, providing mechanistic insights into the reaction dynamics. The QD and QCT models and computational details are given in the Supporting Information (SI).

CH_3Cl has six normal modes: the CH_3 symmetric stretching (ν_1), umbrella (ν_2), CCl stretching (ν_3), CH_3 asymmetric stretching (ν_4), CH_3 asymmetric deforming (ν_5), and CH_3 rocking (ν_6). The 6D Hamiltonian includes the first three modes, that is, (ν_1, ν_2, ν_3), and the computed fundamental frequencies shown in Table 1 indicate good agreement with experiment. In Figure 1b, the QD reaction probabilities (J_{tot} = 0) are shown as a function of collision energy for four selected low-lying vibrational states of CH_3Cl. None has a reaction threshold, consistent with the barrierless reaction pathway with a submerged saddle point (Figure 1a). The reaction

Table 1. Comparison of Calculated and Observed Fundamental Frequencies (cm^{-1}) of the CH_3 Stretching (ν_1), CH_3 Umbrella (ν_2), and CCl Stretching (ν_3) Modes of CH_3Cl along with SVP Values

state	this work	expt.	SVP
(0,0,1)	743	732	0.84
(0,1,0)	1377	1355	0.33
(1,0,0)	3049	2937	0.10

DOI: 10.1021/acs.jpclett.6b01457
J. Phys. Chem. Lett. 2016, 7, 3322−3327

probabilities are all quite large and dependent on the initial reactant vibrational excitation. Interestingly, all reaction probabilities first drop sharply, then increase, and finally decrease gradually with the increase of collision energy.

To gain mechanistic insight into this unusual behavior, the corresponding QCT reaction probabilities were computed with zero impact parameter at five representative collision energies, 0.5, 1.5, 4.0, 8.0, and 11.5 kcal/mol, shown in Figure 1c. It is clear that the total QCT probabilities follow the same trend as the QD counterparts. For the energy range studied here, the reaction is dominated by the Walden-inversion pathway depicted in Figure 1a, with or without formation of the prereaction complex.[13] The corresponding direct and indirect mechanisms have been previously observed for S_N2 reactions.[5] The fractions of direct and indirect trajectories, based on their reaction times,[9] for the ground-state reaction are shown in the same figure. The indirect mechanism dominates at very low energies due apparently to the trapping in the prereaction well. The direct mechanism, on the other hand, increases with collision energy, reaches a maximum near E_{coll}= 4.0 kcal/mol, and then decreases. Because the reaction takes place almost completely following the minimum-energy path, the increasing collision energy enhances the reactivity by avoiding the formation of a prereaction complex. At even higher energies, however, the rapidly moving F^- makes it difficult to capture CH_3Cl. In particular, our results are consistent with the experimental observation for the title reaction that the direct mechanism accounts for ~50% of the yield at 13 kcal/mol.[9]

The change of the reaction mechanism has a strong impact on the mode specificity of the title reaction. In Figure 2a, the reaction probability ratios between the three vibrationally excited CH_3Cl and its ground state are plotted as a function of collision energy. To facilitate discussion of the mode-specific reactivity, we define three regions based on the turning points of the probability curves: region I with collision energies smaller than 1.5 kcal/mol, region II between 1.5 and 4.0 kcal/mol, and region III with larger than 4.0 kcal/mol. In region I, vibrational excitations have a slight inhibitory effect on the reaction for all reactant modes. In region II, however, all vibrational excitations promote the reaction, with the C−Cl stretching excitation offering the strongest enhancement. The mode specificity becomes complicated in region III. The excitation of the C−Cl stretching or CH_3 umbrella mode clearly promotes the reactivity, with the former more strongly, while the excitation of the CH_3 symmetric stretching mode suppresses the reaction. In Figure 2b, the QCT ratios are displayed. Although in qualitative agreement, the QCT ratios are less pronounced (0.9−1.2) than the QD ones (0.85−1.3). Both suggest that the C−Cl stretching mode has a larger promotion effect on the reactivity than the umbrella mode, but the QCT results do not reproduce the inhibitory effect of the CH stretching excitation seen by QD at larger collision energies. This may be due to the zero-point leak issue of the QCT method, resulting in unphysical energy flow from the energetic CH stretching mode to the reaction coordinate. Here, we should emphasize that the above discussion is based on results with zero total angular momentum. The situation may change due to the centrifugal potential at higher total angular momentum values, as shown in the following discussion.

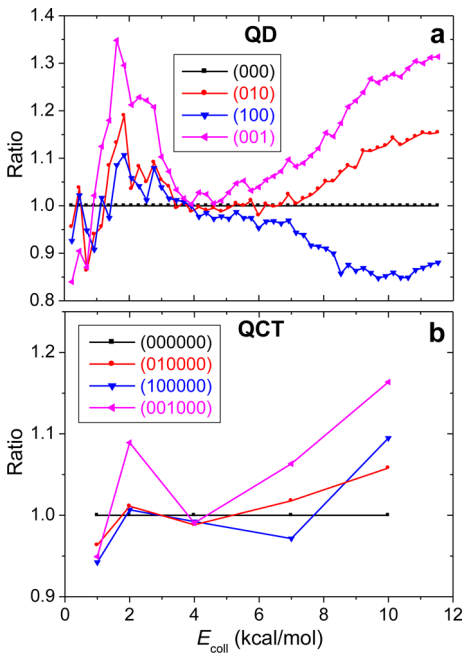

Figure 2. (a) QD and (b) QCT reaction probability ratios between vibrationally excited and ground-state CH_3Cl as a function of collision energy for the F^- + CH_3Cl S_N2 reaction.

The mode specificity discussed above confirms the existence of a nonstatistical component in the title reaction.[59,60] Although the Walden-inversion saddle point is below the reactant asymptote, it still serves as a bottleneck for the reaction. The situation is similar to the H_2O^+ + H_2 reaction, which also has a submerged barrier. The observed rotational enhancement of the reactivity in that reaction[35] was rationalized by the Sudden Vector Projection (SVP) model,[33] which attributes the sudden limit in the reactivity enhancement to a strong coupling with the reaction coordinate at the saddle point.[64,65] To understand the mode specificity here, projections of the three reactant vibrational modes ($\vec{Q}_i$) onto the reaction coordinate of the inversion saddle point ($\vec{Q}_{RC}$), namely, the SVP values $\eta_i = \vec{Q}_i \cdot \vec{Q}_{RC}$, are listed in Table 1 (the SVP values for other vibrational modes are near zero; see the SI). It can be seen that the C−Cl stretch (ν_3) couples to the reaction coordinate the strongest, followed by the CH_3 umbrella (ν_2), while the CH_3 symmetric stretch (ν_1) is only weakly coupled. This is consistent with the elongation of the C−Cl bond and the inversion of the CH_3 group at the C_{3v} saddle point. The strong coupling with the reaction coordinate is expected to lead to enhancement of reactivity in the direct mechanism where the sudden approximation is expected to hold. The predicted promotional effect of these modes by SVP offers an intuitive interpretation of the QD results where the direct mechanism dominates (regions II and III to a lesser extent). On the other hand, the enhancement by the ν_1 mode in the QCT result near 10 kcal/mol is, as discussed in the SI, due to the large contribution of the indirect mechanism in which the energy in the CH_3 stretching mode could conceivably leak (perhaps unphysically) into other DOFs of the reacting system. The overall success of the SVP model confirms in retrospect the adequacy of the 6D model in describing the title reaction as the most important modes are included.

The reaction mechanism also changes with the impact parameter because of the centrifugal potential. Figure 3a shows the QD reaction probabilities for the ground state in several selected partial waves. The probability curves for low total angular momentum (J_{tot}) partial waves have similar characters,

DOI: 10.1021/acs.jpclett.6b01457
J. Phys. Chem. Lett. 2016, 7, 3322−3327

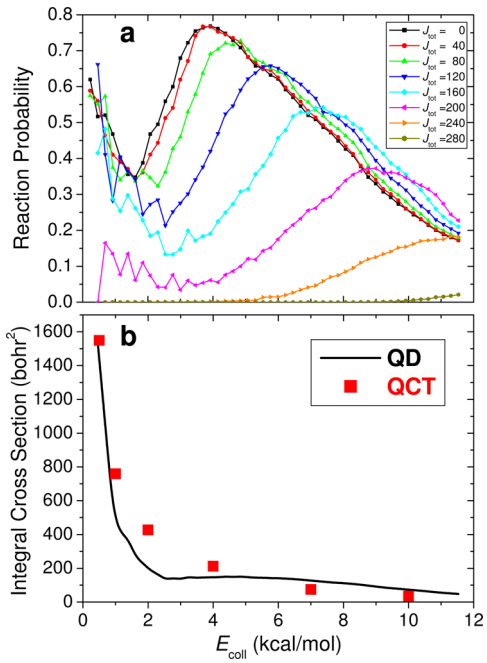

Figure 3. (a) QD reaction probabilities for several selected partial waves and (b) QD and QCT ICSs as a function of collision energy for the ground-state $F^- + CH_3Cl$ S_N2 reaction.

that is, a nonmonotonic energy dependence. However, as J_{tot} increases to 240, the reaction probabilities become monotonically increasing functions with collision energy, analogous to an activated chemical reaction with a well-defined barrier. The corresponding integral cross section (ICS) is plotted in Figure 3b, which decays with collision energy, dictated by the attractive long-range PES leading to the prereaction well. The lower reactivity at high collision energies is attributable to the inefficient capture of the anion, namely, the narrowing of the cone of acceptance. The shape of the excitation function is well reproduced by QCT computations, as also shown in the same figure and consistent with the measured and previously calculated dependence of the rate coefficient on collision energies.[23,60] The QCT results for other excited vibrational modes not included in our 6D QD model are given in the SI, and the implications in mode specificity are discussed there.

Hennig and Schmatz performed time-independent quantum scattering calculations on the $Cl^- + CH_3Cl' \rightarrow CH_3Cl + Cl'^-$ and $Cl^- + CH_3Br \rightarrow CH_3Cl + Br^-$ reactions using a 4D collinear model.[45,47] While the barrier for the symmetric S_N2 reaction is higher than the reactant asymptote, the asymmetric $Cl^- + CH_3Br$ reaction resembles the title reaction. Their results on the latter reaction indicated that for collision energies up to ~7.0 kcal/mol excitation of either the C−Br stretching or CH_3 umbrella mode promotes the reactivity, but the former is more effective, consistent with the findings here above 1.5 kcal/mol. The enhancement of reactivity of the $Cl^- + CH_3Cl'$ reaction by the C−Cl′ excitation has also been reported in earlier QCT and more recent 3D QD studies.[37,50] However, the 4D calculations found that fundamental excitation of the CH_3 stretching mode enhances the reactivity with several orders of magnitude at low collision energies, while it becomes a pure spectator at high collision energies. This is inconsistent with our results, presumably due to the fact that the 4D model only allows collinear collisions. These differences underscore the importance of high-dimensional QD models in describing complex reaction dynamics in S_N2 reactions.

The dynamics of the prototypical gas-phase S_N2 reaction $F^- + CH_3Cl \rightarrow CH_3F + Cl^-$ has been studied using a reduced-dimensional QD model on an accurate global PES. The 6D model includes the most relevant DOFs, enabling a realistic characterization of the most important reaction mechanisms, including both direct and indirect ones. Mechanistic insights are provided by full-dimensional QCT calculations on the same PES, revealing competition between direct and indirect pathways in various energy ranges. Strong mode specificity is found in the direct channel by both QD and QCT calculations. The mode specificity in the direct reaction is rationalized by the SVP model, which attributes the enhancement of reactivity to the coupling of reactant vibrational modes with the reaction coordinate at the submerged saddle point. It is our hope that these theoretical predictions will stimulate experimental exploration of mode-specific reactivity in S_N2 reactions.

■ ASSOCIATED CONTENT

Supporting Information

The Supporting Information is available free of charge on the ACS Publications website at DOI: 10.1021/acs.jpclett.6b01457.

Details of the 6D quantum model, QCT computations, and the SVP model as well as additional results (PDF)

■ AUTHOR INFORMATION

Corresponding Authors

*E-mail: gczako@chem.u-szeged.hu (G.C.).
*E-mail: hguo@unm.edu (H.G.).
*E-mail: yangmh@wipm.ac.cn (M.Y.).

Author Contributions

⊥Y.W. and H.S. contributed equally to this work.

Notes

The authors declare no competing financial interest.

■ ACKNOWLEDGMENTS

M.Y. was supported by the National Natural Science Foundation of China (Project No. 21373266). G.C. was supported by the Scientific Research Fund of Hungary (PD-111900) and the János Bolyai Research Scholarship of the Hungarian Academy of Sciences. H.G. thanks the United States Department of Energy for support (DE-FR02-05ER15694).

■ REFERENCES

(1) Ingold, C. K. *Structure and Mechanisms in Organic Chemistry*; Cornell University Press: Ithaca, NY, 1953.

(2) Chabinyc, M. L.; Craig, S. L.; Regan, C. K.; Brauman, J. I. Gas-Phase Ionic Reactions: Dynamics and Mechanism of Nucleophilic Displacements. *Science* **1998**, *279*, 1882−1886.

(3) Laerdahl, J. K.; Uggerud, E. Gas Phase Nucleophilic Substitution. *Int. J. Mass Spectrom.* **2002**, *214*, 277−314.

(4) Mikosch, J.; Weidemüller, M.; Wester, R. On the Dynamics of Chemical Reactions of Negative Ions. *Int. Rev. Phys. Chem.* **2010**, *29*, 589−617.

(5) Xie, J.; Otto, R.; Mikosch, J.; Zhang, J.; Wester, R.; Hase, W. L. Identification of Atomic-Level Mechanisms for Gas-Phase $X^- + CH_3Y$ S_N2 Reactions by Combined Experiments and Simulations. *Acc. Chem. Res.* **2014**, *47*, 2960−2969.

(6) Mikosch, J.; Trippel, S.; Eichhorn, C.; Otto, R.; Lourderaj, U.; Zhang, J. X.; Hase, W. L.; Weidemuller, M.; Wester, R. Imaging Nucleophilic Substitution Dynamics. *Science* **2008**, *319*, 183−186.

DOI: 10.1021/acs.jpclett.6b01457
J. Phys. Chem. Lett. 2016, 7, 3322−3327

(7) Otto, R.; Brox, J.; Trippel, S.; Stei, M.; Best, T.; Wester, R. Single Solvent Molecules Can Affect the Dynamics of Substitution Reactions. *Nat. Chem.* **2012**, *4*, 534−538.
(8) Mikosch, J.; Zhang, J.; Trippel, S.; Eichhorn, C.; Otto, R.; Sun, R.; de Jong, W. A.; Weidemüller, M.; Hase, W. L.; Wester, R. Indirect Dynamics in a Highly Exoergic Substitution Reaction. *J. Am. Chem. Soc.* **2013**, *135*, 4250−4259.
(9) Stei, M.; Carrascosa, E.; Kainz, M. A.; Kelkar, A. H.; Meyer, J.; Szabó, I.; Czakó, G.; Wester, R. Influence of the Leaving Group on the Dynamics of a Gas-Phase S_N2 Reaction. *Nat. Chem.* **2016**, *8*, 151−156.
(10) Zhang, J.; Mikosch, J.; Trippel, S.; Otto, R.; Weidemüller, M.; Wester, R.; Hase, W. L. $F^- + CH_3I \rightarrow FCH_3 + I^-$ Reaction Dynamics. Nontraditional Atomistic Mechanisms and Formation of a Hydrogen-Bonded Complex. *J. Phys. Chem. Lett.* **2010**, *1*, 2747−2752.
(11) Zhang, J.; Lourderaj, U.; Sun, R.; Mikosch, J.; Wester, R.; Hase, W. L. Simulation Studies of the $Cl^- + CH_3I$ S_N2 Nucleophilic Substitution Reaction: Comparison with Ion Imaging Experiments. *J. Chem. Phys.* **2013**, *138*, 114309.
(12) Xie, J.; Sun, R.; Siebert, M. R.; Otto, R.; Wester, R.; Hase, W. L. Direct Dynamics Simulations of the Product Channels and Atomistic Mechanisms for the $OH^- + CH_3I$ Reaction. Comparison with Experiment. *J. Phys. Chem. A* **2013**, *117*, 7162−7178.
(13) Szabó, I.; Császár, A. G.; Czakó, G. Dynamics of the $F^- + CH_3Cl \rightarrow Cl^- + CH_3F$ S_N2 Reaction on a Chemically Accurate Potential Energy Surface. *Chem. Sci.* **2013**, *4*, 4362−4370.
(14) Szabó, I.; Czakó, G. Revealing a Double-Inversion Mechanism for the F^-+CH_3Cl S_N2 Reaction. *Nat. Commun.* **2015**, *6*, 5972.
(15) Zhang, J.; Xie, J.; Hase, W. L. Dynamics of the $F^- + CH_3I \rightarrow HF + CH_2I^-$ Proton Transfer Reaction. *J. Phys. Chem. A* **2015**, *119*, 12517−12525.
(16) Szabó, I.; Czakó, G. Double-Inversion Mechanisms of the $X^- + CH_3Y$ [X,Y = F, Cl, Br, I] S_N2 Reactions. *J. Phys. Chem. A* **2015**, *119*, 3134−3140.
(17) Olmstead, W. N.; Brauman, J. I. Gas-Phase Nulceophilic Displacement Reactions. *J. Am. Chem. Soc.* **1977**, *99*, 4219−4228.
(18) DePuy, C. H.; Gronert, S.; Mullin, A.; Bierbaum, V. M. Gas-Phase S_N2 and E2 Reactions of Alkyl Halides. *J. Am. Chem. Soc.* **1990**, *112*, 8650−8655.
(19) Xie, J.; Hase, W. L. Rethinking the S_N2 Reaction. *Science* **2016**, *352*, 32−33.
(20) Hase, W. L. Simulations of Gas-Phase Chemical Reactions: Applications to S_N2 Nucleophilic Substitution. *Science* **1994**, *266*, 998−1002.
(21) Sun, L.; Song, K.; Hase, W. L. A S_N2 Reaction That Avoids Its Deep Potential Energy Minimum. *Science* **2002**, *296*, 875−878.
(22) Manikandan, P.; Zhang, J.; Hase, W. L. Chemical Dynamics Simulations of $X^- + CH_3Y \rightarrow XCH_3 + Y^-$ Gas-Phase S_N2 Nucleophilic Substitution Reactions. Nonstatistical Dynamics and Nontraditional Reaction Mechanisms. *J. Phys. Chem. A* **2012**, *116*, 3061−3080.
(23) Su, T.; Morris, R. A.; Viggiano, A. A.; Paulson, J. F. Kinetic Energy and Temperature Dependences for the Reactions of Fluoride with Halogenated Methanes: Experiment and Theory. *J. Phys. Chem.* **1990**, *94*, 8426−8430.
(24) Viggiano, A. A.; Morris, R. A.; Paschkewitz, J. S.; Paulson, J. F. Kinetics of the Gas-Phase Reactions of Chloride Anion, Cl^- with CH_3Br and CD_3Br: Experimental Evidence for Nonstatistical Behavior? *J. Am. Chem. Soc.* **1992**, *114*, 10477−10482.
(25) Graul, S. T.; Bowers, M. T. Vibrational Excitation in Products of Nucleophilic Substitution: The Dissociation of Metastable $X^-(CH_3Y)$ in the Gas Phase. *J. Am. Chem. Soc.* **1994**, *116*, 3875−3883.
(26) DeTuri, V. F.; Hintz, P. A.; Ervin, K. M. Translational Activation of the S_N2 Nucleophilic Displacement Reactions $Cl^- + CH_3Cl$ $(CD_3Cl) \rightarrow ClCH_3$ $(ClCD_3) + Cl^-$: A Guided Ion Beam Study. *J. Phys. Chem. A* **1997**, *101*, 5969−5986.
(27) Ayotte, P.; Kim, J.; Kelley, J. A.; Nielsen, S. B.; Johnson, M. A. Photoactivation of the $Cl^-+ CH_3Br$ S_N2 Reaction Via Rotationally Resolved C−H Stretch Excitation of the $Cl^-\cdot CH_3Br$ Entrance Channel Complex. *J. Am. Chem. Soc.* **1999**, *121*, 6950−6951.
(28) Tonner, D. S.; McMahon, T. B. Non-Statistical Effects in the Gas Phase S_N2 Reaction. *J. Am. Chem. Soc.* **2000**, *122*, 8783−8784.
(29) Angel, L. A.; Ervin, K. M. Dynamics of the Gas-Phase Reactions of Fluoride Ions with Chloromethane. *J. Phys. Chem. A* **2001**, *105*, 4042−4051.
(30) Crim, F. F. Vibrational State Control of Bimolecular Reactions: Discovering and Directing the Chemistry. *Acc. Chem. Res.* **1999**, *32*, 877−884.
(31) Crim, F. F. Chemical Dynamics of Vibrationally Excited Molecules: Controlling Reactions in Gases and on Surfaces. *Proc. Natl. Acad. Sci. U. S. A.* **2008**, *105*, 12654−12661.
(32) Czakó, G.; Bowman, J. M. Reaction Dynamics of Methane with F, O, Cl, and Br on Ab Initio Potential Energy Surfaces. *J. Phys. Chem. A* **2014**, *118*, 2839−2864.
(33) Guo, H.; Jiang, B. The Sudden Vector Projection Model for Reactivity: Mode Specificity and Bond Selectivity Made Simple. *Acc. Chem. Res.* **2014**, *47*, 3679−3685.
(34) Li, J.; Jiang, B.; Song, H.; Ma, J.; Zhao, B.; Dawes, R.; Guo, H. From Ab Initio Potential Energy Surfaces to State-Resolved Reactivities: The $X + H_2O \leftrightarrow HX + OH$ (X = F, Cl, and $O(^3P)$) Reactions. *J. Phys. Chem. A* **2015**, *119*, 4667−4687.
(35) Xu, Y.; Xiong, B.; Chang, Y. C.; Ng, C. Y. Communication: Rovibrationally Selected Absolute Total Cross Sections for the Reaction $H_2O^+(X^2B_1; v_1^+v_2^+v_3^+ = 000; N^+_{Ka^+Kc^+}) + D_2$: Observation of the Rotational Enhancemeent Effect. *J. Chem. Phys.* **2012**, *137*, 241101.
(36) Viggiano, A. A.; Morris, R. A. Rotational and Vibrational Energy Effects on Ion−Molecule Reactivity as Studied by the VT-SIFDT Technique. *J. Phys. Chem.* **1996**, *100*, 19227−19240.
(37) Vande Linde, S. R.; Hase, W. L. A Direct Mechanism for S_N2 Nucleophilic Substitution Enhanced by Mode-Selective Vibrational Excitation. *J. Am. Chem. Soc.* **1989**, *111*, 2349−2351.
(38) Schmatz, S. Quantum Dynamics of Gas-Phase S_N2 Reactions. *ChemPhysChem* **2004**, *5*, 600−617.
(39) Hase, W. L. Classical Trajectory Simulations: Initial Conditions. In *Encyclopedia of Computational Chemistry*; Alinger, N. L., Ed.; Wiley: New York, 1998; pp 399−402.
(40) Clary, D. C.; Palma, J. Quantum Dynamics of the Walden Inversion Reaction $Cl^-+CH_3Cl \rightarrow ClCH_3+Cl^-$. *J. Chem. Phys.* **1997**, *106*, 575−583.
(41) Wang, H.; Goldfield, E. M.; Hase, W. L. Quantum Dynamical Study of the Cl^-+CH_3Br S_N2 Reaction. *J. Chem. Soc., Faraday Trans.* **1997**, *93*, 737−746.
(42) Schmatz, S.; Clary, D. C. Quantum Scattering on S_N2 Reactions: Influence of Azimuthal Rotations. *J. Chem. Phys.* **1998**, *109*, 8200−8217.
(43) Yu, H.-G.; Nyman, G. An Application of the Rotating Line Umbrella Model to Quantum Dynamics of S_N2 Reactions. *Chem. Phys. Lett.* **1999**, *312*, 585−590.
(44) Schmatz, S.; Hauschildt, J. Four-Mode Calculation of Resonance States of Intermediate Complexes in the S_N2 Reaction $Cl^-+CH_3Cl' \rightarrow ClCH_3+Cl'^-$. *J. Chem. Phys.* **2003**, *118*, 4499−4516.
(45) Hennig, C.; Schmatz, S. State-Selected Dynamics of the Complex-Forming Bimolecular Reaction $Cl^-+CH_3Cl' \rightarrow ClCH_3+Cl'^-$: A Four-Dimensional Quantum Scattering Study. *J. Chem. Phys.* **2004**, *121*, 220−236.
(46) Schmatz, S. Four-Mode Quantum Calculations of Resonance States in Complex-Forming Bimolecular Reactions: Cl^-+CH_3Br. *J. Chem. Phys.* **2005**, *122*, 234306.
(47) Hennig, C.; Schmatz, S. Four-Dimensional Quantum Study on Exothermic Complex-Forming Reactions: $Cl^-+CH_3Br \rightarrow ClCH_3+Br^-$. *J. Chem. Phys.* **2005**, *122*, 234307.
(48) Hennig, C.; Schmatz, S. Rotational Effects in Complex-Forming Bimolecular Substitution Reactions: A Quantum-Mechanical Approach. *J. Chem. Phys.* **2009**, *131*, 224303.
(49) Hennig, C.; Schmatz, S. Differential Reaction Cross Sections from Rotationally Resolved Quantum Scattering Calculations: Application to Gas-Phase S_N2 Reactions. *Phys. Chem. Chem. Phys.* **2012**, *14*, 12982−12991.

DOI: 10.1021/acs.jpclett.6b01457
J. Phys. Chem. Lett. 2016, 7, 3322−3327

(50) Kowalewski, M.; Mikosch, J.; Wester, R.; de Vivie-Riedle, R. Nucleophilic Substitution Dynamics: Comparing Wave Packet Calculations with Experiment. *J. Phys. Chem. A* **2014**, *118*, 4661−4669.
(51) Palma, J.; Clary, D. C. A Quantum Model Hamiltonian to Treat Reactions of the Type X + YCZ_3 → XY + CZ_3: Application to $O(^3P)$ + CH_4 → OH + CH_3. *J. Chem. Phys.* **2000**, *112*, 1859−1867.
(52) Yang, M.; Lee, S.-Y.; Zhang, D. H. Seven-Dimensional Quantum Dynamics Study of the $O(^3P)$+CH_4 Reaction. *J. Chem. Phys.* **2007**, *126*, 064303.
(53) Zhang, W.; Zhou, Y.; Wu, G.; Lu, Y.; Pan, H.; Fu, B.; Shuai, Q.; Liu, L.; Liu, S.; Zhang, L.; Jiang, B.; Dai, D.; Lee, S.-Y.; Xie, Z.; Braams, B. J.; Bowman, J. M.; Collins, M. A.; Zhang, D. H.; Yang, X. Depression of Reactivity by the Collision Energy in the Single Barrier H + CD_4 → HD + CD_3 Reaction. *Proc. Natl. Acad. Sci. U. S. A.* **2010**, *107*, 12782−12785.
(54) Liu, R.; Xiong, H.; Yang, M. An Eight-Dimensional Quantum Mechanical Hamiltonian for X+YCZ_3 System and Its Applications to H+CH_4 Reaction. *J. Chem. Phys.* **2012**, *137*, 174113.
(55) Liu, R.; Yang, M.; Czakó, G.; Bowman, J. M.; Li, J.; Guo, H. Mode Selectivity for a "Central" Barrier Reaction: Eight-Dimensional Quantum Studies of the $O(^3P)$ + CH_4 → OH + CH_3 Reaction on an Ab Initio Potential Energy Surface. *J. Phys. Chem. Lett.* **2012**, *3*, 3776−3780.
(56) Liu, R.; Wang, F.; Jiang, B.; Czakó, G.; Yang, M.; Liu, K.; Guo, H. Rotational Mode Specificity in the Cl + CHD_3 → HCl + CD_3 Reaction. *J. Chem. Phys.* **2014**, *141*, 074310.
(57) Liu, N.; Yang, M. An Eight-Dimensional Quantum Dynamics Study of the Cl + CH_4→ HCl + CH_3 Reaction. *J. Chem. Phys.* **2015**, *143*, 134305.
(58) Qi, J.; Song, H.; Yang, M.; Palma, J.; Manthe, U.; Guo, H. Communication: Mode Specific Quantum Dynamics of the F + CHD_3 → HF + CD_3 Reaction. *J. Chem. Phys.* **2016**, *144*, 171101.
(59) Wang, H.; Hase, W. L. Kinetics of F^- + CH_3Cl S_N2 Nucleophilic Substitution. *J. Am. Chem. Soc.* **1997**, *119*, 3093−3102.
(60) Su, T.; Wang, H.; Hase, W. L. Trajectory Studies of S_N2 Nucleophilic Substitution. 7. F^- + CH_3Cl → FCH_3 + Cl^-. *J. Phys. Chem. A* **1998**, *102*, 9819−9828.
(61) Gonzales, J. M.; Pak, C.; Cox, R. S.; Allen, W. D.; Schaefer, H. F., III; Császár, A. G.; Tarczay, G. Definitive Ab Initio Studies of Model S_N2 Reactions CH_3X+F^- (X = F, Cl, CN, OH, SH, NH_2, PH_2). *Chem. - Eur. J.* **2003**, *9*, 2173−2192.
(62) Zhang, J.; Xu, Y.; Chen, J.; Wang, D. A Multilayered-Representation, Quantum Mechanical/Molecular Mechanics Study of the CH_3Cl + F^- Reaction in Aqueous Solution: The Reaction Mechanism, Solvent Effects and Potential of Mean Force. *Phys. Chem. Chem. Phys.* **2014**, *16*, 7611−7617.
(63) Szabó, I.; Czakó, G. Rotational Mode Specificity in the F^- + CH_3Y [Y = F and Cl] S_N2 Reactions. *J. Phys. Chem. A* **2015**, *119*, 12231−12237.
(64) Li, A.; Guo, H. A Nine-Dimensional Ab Initio Global Potential Energy Surface for the H_2O^+ + H_2 → H_3O^+ + H Reaction. *J. Chem. Phys.* **2014**, *140*, 224313.
(65) Song, H.; Li, A.; Guo, H.; Xu, Y.; Xiong, B.; Chang, Y. C.; Ng, C. Comparison of Experimental and Theoretical Quantum-State-Selected Integral Cross Sections for the H_2O^+ + H_2 (D_2) Reactions in the Collision Energy Range of 0.04−10.00 eV. *Phys. Chem. Chem. Phys.* **2016**, *18*, 22509−22515.

DOI: 10.1021/acs.jpclett.6b01457
J. Phys. Chem. Lett. 2016, 7, 3322−3327